

ESTIMATING THE DISTRIBUTION OF 3D GENERALIZED CYLINDERS ANGLES FROM AN IMAGE

Jean-Pierre Da Costa, Stefan Oprean, Pierre Baylou, Christian Germain

Univ. Bordeaux, IMS UMR 5218, F-33400 Talence, France
CNRS, IMS, UMR 5218, F-33400 Talence, France

ABSTRACT

The use of 3D imaging techniques is a choice approach for the study of the inner structure of materials. However, for large industrial applications, the stereological analysis of 2D snapshots of material sections is still necessary for obvious time and cost reasons. We present a novel method to analyze the 3D layout of cylindrical structures from a single 2D section. In particular we propose to estimate the distribution of cutting angles i.e. angles between the cylinders axis and the normal to the image plane. Contrary to existing approaches, the knowledge of the cylinder cross section shape is not a prerequisite. The only required input is the statistical distribution of the cylinder cross section area. Our approach is based on the minimization of a least squares criterion under linear constraints. It is evaluated on synthetic data and applied to microscopy images of fibrous composites. Our experimental study focuses on the capabilities and limitations of the approach.

Index Terms— microscopy, stereology, cylinder, orientation, fibrous structures

1. INTRODUCTION

In material science, exploring the three dimensional structure of materials is essential to understand and predict their physical properties and behavior. In the case of composite structures, parameters of interest are for instance the volume ratio, the shapes, the sizes and the spatial distribution of the objects composing the material. In particular, the mechanical properties of woven fibrous composites closely depend on the actual 3D layout of its fibers. Even if fiber layout is meant to be consistent with the nominal manufacturing process, it may show some discrepancies in practice and has to be controlled by artificial vision. Although 3D imaging techniques like tomography or ultrasounds can provide direct descriptions of the material volume, such imaging techniques may be too expensive and not technically appropriate in many cases. For instance, when imaging composite structures at microscopic scale, the use of tomography requires a compromise between resolution and sample size, while optical microscopy or electron microscopy are much easier to use in practice. Confocal microscopy [1] also allows to obtain 3D images of a material but

its use requires expensive equipment and implies drastic sample preparation. Another simple approach that does not need 3D imaging is the *dissector* [2, 3], a stereological technique based on the observation of thin parallel contiguous slices of the material. However, obtaining perfectly parallel slices of an acceptable thickness is quite laborious in practice.

It is also possible to get valuable information about 3D materials from a single 2D image. Stereological techniques allow to extract 3D quantitative measurements from plane sections, especially in the case of simple geometric objects such as spheres, ellipsoids or cylinders [4, 5]. When dealing with anisotropic structures, even 3D orientation can be deduced from 2D. For instance, in the case of fiber composites [6] or cubic metallic structures [7, 8], hypotheses about the shape and spatial distribution of objects allow to relate 3D geometry to the shape and spatial layout of 2D sections.

In this paper, we are interested in fibrous structures that can be modelled by generalized cylinders with arbitrary shape. We aim at analyzing their 3D layout from 2D. More precisely, we want to estimate their *cutting angle* i.e. the angle formed between their 3D axis and the normal to the cutting plane. The relation between the cutting angle and the 2D section shape is well known when the cylinder basis is circular [6]. Indeed, in this case, the cylinder section is an ellipse the geometry of which brings information about the cutting angle and the orientation of the cylinder axis [6, 9].

Things get worse when the cylinder basis is not circular since, in the general case, it is difficult to predict the shape of the cylinder section in 2D when it is cut at an arbitrary orientation. As a consequence, it is almost impossible to deduce individual cylinder axis orientation except in some simple specific cases. In this paper, we argue that it is possible to deduce the statistical distribution of cutting angles from the distribution of the areas observed on an oblique section. This can be done, whatever the shapes of the cylinder bases, if the statistical distribution of basis areas is known.

In section 2, we describe the theoretical background of the proposed approach. In section 3, it is validated by means of experiments performed on theoretical distributions and synthetic data. In section 4, we apply the procedure to the estimation of fiber cutting angles in fibrous composites observed in 2D. Finally, we give a few conclusions and prospects.

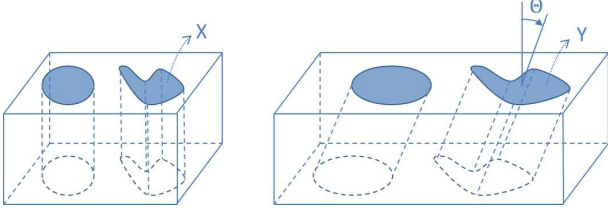


Fig. 1. Cross and oblique sections of a circular and a generalized cylinder. X and Y denote the area of the cross and the oblique sections. Θ is the *cutting angle*.

2. THEORETICAL BACKGROUND

2.1. Definitions

Generalized cylinders refer to cylinders with arbitrary cross section, i.e. with non trivial shapes such as circles, ellipses or rectangles. We will call *oblique section*, the curve of intersection between the cylinder and an arbitrary cutting plane. If the cutting angle is different from $\pi/2$ then the oblique section is closed and its area is finite. Let C be a random generalized cylinder, cut by an arbitrary plane. Let X and Y be two real valued positive random variables that represent the areas of the cross and oblique sections of C . Let $\Theta \in [0, \frac{\pi}{2}[$ represent the cutting angle, as depicted in figure 1 and $Z = \cos \Theta \in]0, 1]$ its cosine. These variables are linked by a simple geometric relation since $Y = \frac{X}{Z}, \forall Z \in]0, 1]$.

Let $F_X(x) = P(X < x)$ be the cumulative distribution function of X and $p_X(x) = \frac{d}{dx}F_X(x)$ its probability density function. In the same way, let $p_Y, p_\Theta, p_Z, F_Y, F_\Theta$ and F_Z be the probability density functions and cumulative distribution functions of Y, Θ and Z .

2.2. Relating probability density functions

Let us start from the expression of the cumulative:

$$F_Y(y) = P(Y < y) = P\left(\frac{X}{Z} < y\right) = P(X < yZ) \quad (1)$$

Conditioning on Z , it follows:

$$F_Y(y) = \int_0^1 P(X < yz | Z = z) p_Z(z) dz \quad (2)$$

As one can reasonably assume that the cosine Z of the cutting angle and the cross section area X are independent, the previous expression becomes:

$$F_Y(y) = \int_0^1 P(X < yz) p_Z(z) dz = \int_0^1 F_X(yz) p_Z(z) dz \quad (3)$$

Deriving F_Y , we get:

$$\begin{aligned} p_Y(y) &= \frac{d}{dy} F_Y(y) = \int_0^1 \frac{\partial}{\partial y} F_X(yz) p_Z(z) dz \quad (4) \\ &= \int_0^1 z F'_X(yz) p_Z(z) dz = \int_0^1 z p_X(yz) p_Z(z) dz \end{aligned}$$

Suppose that the densities of X and Y are known, then looking for the density of the cutting angles is thus equivalent to finding a solution f to the following differential equation:

$$p_Y(y) = \int_0^1 z p_X(yz) f(z) dz, \quad \forall y \in \mathbb{R}^+ \quad (5)$$

with the double constraint $f(z) \geq 0$ and $\int_0^1 f(z) dz = 1$.

2.3. Solving the differential equation

2.3.1. A constrained optimization problem

Equation 5 could be solved as a constrained optimization problem over a function space. The solution could be looked for as a real positive function $f : [0, 1] \rightarrow \mathbb{R}^+$ with unit integral, i.e. a probability density function. A possible optimization criterion $\Phi(f)$ to be minimized should measure how much $\int_0^1 z p_X(yz) f(z) dz$ is in adequacy with $p_Y(y)$, supposedly known or estimated. $\Phi(f)$ could be any measure of similarity between probability density functions.

However, this optimization problem is difficult to address as it is hardly possible to choose a function space in which to perform the optimization without any a priori about the distributions of cutting angles. Besides, in practice, the distribution of oblique section areas is not known analytically. However it can be easily approximated by a discrete histogram.

2.3.2. Discretization of the density functions

Let $h_Y = (h_{Y,1}, \dots, h_{Y,M})^t$ be the discrete histogram of variable Y , i.e. the discretization of p_Y into M intervals:

$$h_{Y,k} = \int_{y_k}^{y_{k+1}} p_Y(y) dy, \quad \forall k \in \{1, \dots, M\} \quad (6)$$

where $y_k \leq y_{k+1}$, $y_1 = 0$ and $y_{M+1} = \infty$. The operator t denotes the matrix transpose.

p_Z can also be discretized into N classes, yielding vector $h_Z = (h_{Z,1}, \dots, h_{Z,N})^t$:

$$h_{Z,l} = \int_{z_l}^{z_{l+1}} p_Z(z) dz, \quad \forall l \in \{1, \dots, N\} \quad (7)$$

with $z_l \leq z_{l+1}$, $z_1 = 0$ and $z_{N+1} = 1$. Then, it comes:

$$\begin{aligned} h_{Y,k} &= \int_{y_k}^{y_{k+1}} \int_0^1 z p_X(yz) p_Z(z) dz dy \\ &= \int_{y_k}^{y_{k+1}} \left[\sum_{l=1}^N \int_{z_l}^{z_{l+1}} z p_X(yz) p_Z(z) dz \right] dy. \quad (8) \end{aligned}$$

If the interval $[z_l, z_{l+1}]$ is small enough, $p_Z(z)$ can be considered to be constant over the interval, that is:

$$p_Z(z) \approx h_{Z,l}/(z_{l+1} - z_l), \quad \forall z \in [z_l, z_{l+1}]. \quad (9)$$

Rewriting equation 8, it appears that the discrete values $h_{Y,k}$ are linked linearly to the discrete values $h_{Z,l}$:

$$h_{Y,k} \approx \sum_{l=1}^N h_{Z,l} b_{k,l} \quad (10)$$

with $b_{k,l} = \frac{1}{z_{l+1} - z_l} \int_{y_k}^{y_{k+1}} \int_{z_l}^{z_{l+1}} z p_X(yz) dz dy$.

2.3.3. Least squares formulation

In practice, the discrete distribution of oblique section areas h_Y is unknown but is estimated from a statistical sample (from an image). Let $\hat{h}_Y = (\hat{h}_{Y,1}, \dots, \hat{h}_{Y,M})^t$ be its estimate. Besides, if the distribution of cross section areas p_X is known, the coefficients $b_{k,l}$ can be calculated or numerically approximated. Our optimization problem can thus be expressed as the search of a distribution $\hat{h}_Z = (\hat{h}_{Z,1}, \dots, \hat{h}_{Z,N})^t$ so that:

$$\hat{h}_{Y,k} \approx \sum_{l=1}^N \hat{h}_{Z,l} b_{k,l} \quad \forall k \in \{1, \dots, M\}. \quad (11)$$

When choosing the least squares criterion, the searched distribution $\hat{h}_Z = (\hat{h}_{Z,1}, \dots, \hat{h}_{Z,N})^t$ is the solution of the constrained optimization problem:

$$\hat{h}_Z = \arg \min_{r_1, \dots, r_N} \sum_{k=1}^M \left(\hat{h}_{Y,k} - \sum_{l=1}^N r_l b_{k,l} \right)^2 \quad (12)$$

with $\sum_{l=1}^N r_l = 1$ and $r_l \geq 0, \forall l$. In other words:

$$\hat{h}_Z = \arg \min_{R \in [0,1]^N} \|h_Y - BR\|^2 \quad (13)$$

$$\text{with } B = \begin{pmatrix} b_{1,1} & \dots & b_{1,N} \\ \vdots & b_{k,l} & \vdots \\ b_{M,1} & \dots & b_{M,N} \end{pmatrix} \text{ and } R = \begin{pmatrix} r_1 \\ \vdots \\ r_N \end{pmatrix},$$

under the constraints $\sum_{l=1}^N r_l = 1$ and $r_l \geq 0, \forall l$.

This quadratic optimization problem with linear equality and inequality constraints can be solved using standard algorithmic solutions.

3. EXPERIMENTAL VALIDATION

3.1. Experimental design

The proposed approach has been validated at two levels. Level 1 focuses on the validation of the optimization process, trying to assess whether the simplification in equation 9 is relevant or not and if parameters M and N have a critical

influence on the cutting angle distribution estimation. In order to answer these questions regardless of image digitization effects and area estimation errors, the experimental validation is based upon numerical computation. Given p_Θ the distribution of the cutting angles and p_X the distribution of the cross section areas, we compute numerically p_Z , p_Y , B and the theoretical discrete distributions h_Z^{th} and h_Y^{th} . B and h_Y^{th} are then fed into the optimization solver (see Eq. (13)) which brings the estimate \hat{h}_Z^{th} that can be compared with h_Z^{th} .

Level 2 has to deal with statistical sampling and image synthesis. It aims at evaluating the effect of statistical sampling and digitization. p_X and p_Θ are sampled L times. The samples are used to produce synthetic 2D images that simulate the oblique section of a collection of generalized cylinders. The produced binary images are labelled into various objects the areas of which are split into classes yielding vector h_Z^{img} and h_Y^{img} . h_Y^{img} is fed into the optimization solver. Its solution \hat{h}_Z^{img} is finally compared with h_Z^{th} . For simplicity and without loss of generality, we have simulated circular cylinders since 2D sections can be easily simulated by drawing ellipses in an image i.e. without generating 3D data.

In our experiments, cross section areas are assumed to follow a known normal distribution: $X \sim \mathcal{N}(\mu_X, \sigma_X)$. Though arbitrary, this hypothesis proves to be relevant in practical cases (see section 4) and allows to ease the computation of matrix B . However, any other distribution can be considered provided that an analytic form or a close approximation is available. For the cutting angles, we considered a wrapped normal distribution $\mathcal{WN}(\mu_\theta, \sigma_\theta)$.

The proposed optimization process provides with the estimated discrete cosine distribution \hat{h}_Z which minimizes the least squares criterion. We plotted a direct measure of the adequacy between \hat{h}_Z and h_Z using the error function:

$$E(h_Z, \hat{h}_Z) = \sum_{n=1}^N |h_{Z,n} - \hat{h}_{Z,n}|. \quad (14)$$

Various values are tested for the histogram bin numbers M (from 30 to 60) and N (from 1 to M). The intervals for the area and for the angle distributions are of equal width.

3.2. Results

Figure 2 illustrates the validation results obtained by feeding the optimization algorithm with a discrete distribution h_Y^{th} computed numerically from a reference cross section distribution and a reference cutting angle distribution. Input cross sections follow a normal distribution $N(548, 139)$. Input cutting angles Θ follow a wrapped normal distribution $\mathcal{WN}(0.2, 0.3)$. $N = 6$ and $M = 30$ bins are used for cosines and area distributions. The theoretical and estimated distributions \hat{h}_Z^{th} and h_Z^{th} are very similar. Only small differences can be noticed regarding the two intervals $\Theta \in [0, \frac{\pi}{6}[$ and $[\frac{\pi}{6}, \frac{\pi}{3}[$ (i.e. $Z \in [\cos \frac{\pi}{3}, \cos \frac{\pi}{6}]$ and $[\cos \frac{\pi}{6}, 1]$). As well, the fit between $\hat{h}_Y^{th} = B\hat{h}_Z^{th}$ and h_Y^{th} appears to be almost perfect.

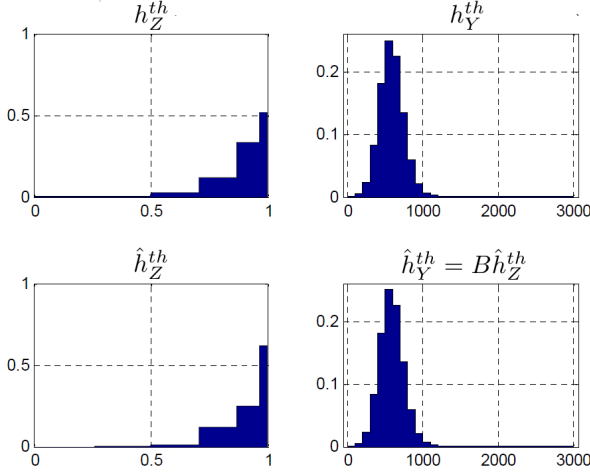


Fig. 2. Comparison of input (h_Z^{th} and h_Y^{th}) and output (\hat{h}_Z^{th} and $\hat{h}_Y^{th} = B\hat{h}_Z^{th}$) distributions at validation level 1. Input cutting angles Θ follow a wrapped normal distribution $\mathcal{WN}(0.2, 0.3)$. Input cross sections follow a normal distribution $N(548, 139)$. Other parameters are $N = 6$ and $M = 30$. Abscissa units for area distributions h_Y^{th} and \hat{h}_Y^{th} are in pixels.

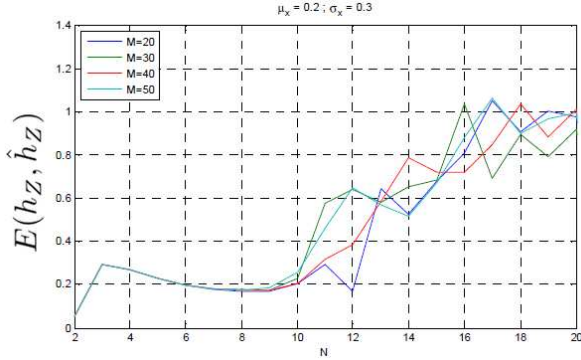


Fig. 3. Plot of the error function $E(h_Z, \hat{h}_Z)$ for various bin number values N and M . Input cutting angles Θ follow a wrapped normal distribution $\mathcal{WN}(0.2, 0.3)$. Input cross sections follow a normal distribution $N(548, 139)$.

In figure 3, we plot the error $E(h_Z^{th}, \hat{h}_Z^{th})$ as a function of N , the number of bins of the angle and cosine histograms, and M the number of bins in the oblique section area histograms. While M has not a strong influence (except for large values of N), it is shown that the quality of the estimation depends strongly on N . The best results are obtained with moderate values for N , between 6 and 9. Though these curves relate to a specific angle distribution $\mathcal{WN}(0.2, 0.3)$, similar results have been obtained with other means and standard deviations.

The second validation stage is carried out using synthetic images that simulate the section of 3D cylindrical structures. The output angle distribution, not shown here, is very similar

in shape to the input theoretical distribution. Table 1 confirms both the excellent match between the observed and the estimated area distributions (i.e. h_y^{img} and $\hat{h}_y^{img} = B\hat{h}_z^{img}$) and the good fit between the input theoretical distribution and its estimation (i.e. h_z^{th} and \hat{h}_z^{img}).

μ_θ	0.1	0.1	0.2	0.2	0.3	0.3
σ_θ	0.1	0.3	0.1	0.3	0.1	0.3
$E(h_Z^{th}, \hat{h}_Z^{img})$	0.10	0.10	0.10	0.10	0.10	0.10

Table 1. Validation at level 2: Error values $E(h_Z^{th}, \hat{h}_Z^{img})$ for various angle distributions $\mathcal{WN}(\mu_\theta, \sigma_\theta)$. Each value is the mean of 100 samples of size 2196.

4. APPLICATION TO MICROSCOPY IMAGES OF WOVEN COMPOSITE MATERIALS

The approach developed in this paper was applied to images of fibrous composite structures. These structures are made of threads containing around a thousand fibers. These threads lie in three orthogonal directions that we will call X, Y and Z. Threads in the Z direction are of great importance as regards the composite robustness. Detecting and counting Z fibers through microscopy imaging has thus become a routine operation for process monitoring. Material samples are imaged more or less orthogonally to the Z fibers. Z fiber sections appear as compact patterns the shape of which depend on the cutting angle but also on the initial morphology of the fibers. Figure 4 shows two sections of such fibrous material. In the first one, the fibers are almost perfectly orthogonal to the image plane whereas, in the second one, they are cut with arbitrary angles. The cross sections have clearly a non circular shape. Oblique sections appear to have even more complex shapes. Although these shapes clearly depend on the cutting angle and on individual fiber directions, no simple geometric relation has yet been established. Better than trying to estimate individual cutting angles, we estimated the global cutting angle distribution by applying our method.

As a prerequisite of the method is to know the distribution of fiber cross section areas, a set of images of orthogonal views of fiber bundles were acquired using an optical microscope. More than 2,300 fiber sections were segmented and analyzed to estimate the mean and standard deviation of the distribution. The normality assumption appeared to be relevant.

The inversion algorithm was applied to a set of images comprising more than 30,000 fibers. Fibers that were cut longitudinally were removed a priori during the image segmentation and classification process. The distribution of the remaining fibers cutting angles i.e. the angular deviates of fibers from the normal of the image plane is reported in figure 5. Z fibers are defined by material specialists as fibers that are less than a given angle θ_{max} apart from the normal

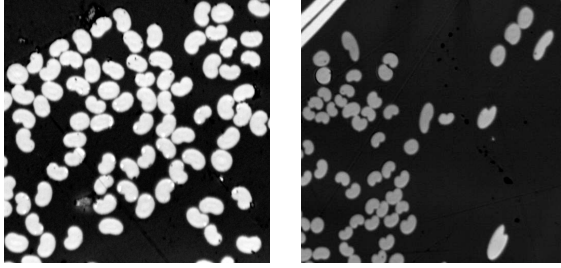


Fig. 4. Micrographs of carbon fibers. Left: fibers are observed orthogonally, the cross sections show specific *bean* shapes. Right: individual fibers are cut at an arbitrary angle, the oblique section are of varying non trivial shapes.

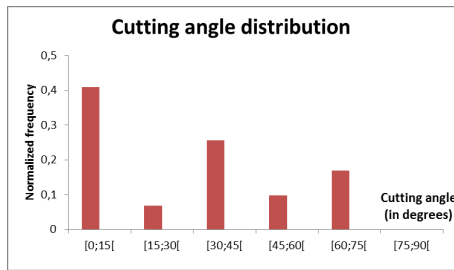


Fig. 5. Example of a cutting angle distribution obtained with the proposed approach from the cross and oblique section distributions of an experimental set of images comprising a total of more than 30,000 fibers.

to the weaving plane. As the weaving plane corresponds approximately to the image plane, the Z fiber count is obtained by summing the histogram bins related to angles smaller than θ_{max} , which is direct.

5. CONCLUSION

In this paper, we presented a novel method for the analysis of the 3D spatial layout of generalized cylindrical structures from a single section image. This method estimates the distribution of the cutting angles i.e. the angles between the cylinder axis and the normal to the image plane. Contrary to existing approaches, the method is not tied to the shape of cylinder bases and can be applied to structures of arbitrary shapes. The only prerequisite is the knowledge of the cross section area distribution. It hinges on the discretization of area and angle distributions and on the minimization of a least square criterion carried out with standard quadratic optimization solvers.

An experimental evaluation was conducted on synthetic data which showed the capabilities of the approach. Finally, the proposed algorithm was applied in an industrial context to the estimation of cutting angles from images of 3D fibrous structures. Once again, the capabilities of the approach were evaluated.

In future works, a thorough study of the sensitivity of the

approach to deviations from the model will be carried out, both on synthetic and experimental images. For instance, we will study the sensitivity of the approach to deviations from the normal distribution or to errors in the estimation of the mean and variance .

6. REFERENCES

- [1] C. Eberhardt and A. Clarke, "Fiber-orientation measurements in short-glass-fibre composites. part i. automated, high-angular-resolution measurement by confocal microscopy," *Composites Science and Technology*, vol. 61, no. 10, pp. 1389–1400, 2001.
- [2] D.C. Sterio, "The unbiased estimation of number and sizes of arbitrary particles using the disector.," *Journal of Microscopy*, vol. 134, no. 2, pp. 127–136, 1984.
- [3] N.C. Davidson, A.R. Clarke, and G. Archetypal, "Large-area, high-resolution image analysis of composite materials," *Journal of Microscopy*, vol. 185, no. 2, pp. 233–242, 1997.
- [4] J.C. Russ and R.T. Dehoff, *Practical Stereology*, New York: Plenum Press, 2000.
- [5] R. B. S. Oakeshott and S. F. Edwards, "On the stereology of ellipsoids and cylinders," *Physica A: Statistical Mechanics and its Applications*, vol. 189, no. 12, pp. 208–233, 1992.
- [6] R. Blanc, C. Germain, J.-P. Da Costa, P. Baylou, and M. Cataldi, "Fiber orientation measurements in composite materials," *Composites Part A*, vol. 37, no. 2, pp. 197–206, 2006.
- [7] C. Germain, R. Blanc, M. Donias, O. Lavialle, J.-P. Da Costa, and P. Baylou, "Estimating the section elevation angle of cubes on a cubic mesh. application to nickel microstructure size estimation," *Image Analysis & Stereology*, vol. 24, no. 3, pp. 127–134, 2005.
- [8] R. Blanc, P. Baylou, C. Germain, and J.-P. Da Costa, "Confidence bounds for the estimation of the volume phase fraction from a single image in a nickel base superalloy," *Microscopy and Microanalysis*, vol. 16, no. 03, pp. 273–281, 2010.
- [9] B. Mlekusch, "Fiber orientation in short-fiber-reinforced thermoplastics. ii. quantitative measurements by image analysis.," *Composites Science and Technology*, vol. 59, no. 4, pp. 547–560, 1999.